

3-D Inverse Radon Transform by Use of Tree-Structured Filter Bank

Yoshitaka MORIKAWA¹ and Junichi MURAKAMI²

¹ Department of Communication Network Engineering,
Faculty of Engineering, Okayama University,
3-1-2 Tsusimanaka, Okayama-city, Okayama 700-8530, Japan
Tel. +86-251-8126, Fax.: +86-251-8127
e-mail :morikawa@cne.okayama-u.ac.jp

² Department of Control Engineering, Takuma National College of Technology,
551 Kouda, Takuma-cho, Mitoyo-gun, Kagawa, 769-1192, Japan

Abstract: Two-dimensional (2-D) X-ray computerized tomography (CT) equipments are widely used in industrial and medical fields, and nowadays studies on reconstruction algorithm for 3-D cone-beam acquisition systems are active for better utilization. The authors recently have proposed a fast reconstruction algorithm using tree-structured filter bank for 2-D CT, and shown the algorithm is applicable to an approximate reconstruction of 3-D CT. For exact 3-D CT reconstruction, however, we have to backproject 1-D signal into 3-D space. This paper proposes a fast implementation method for this back-projection by use of tree-structured filter bank, and shows the proposed method works approximately 700 times faster than the direct one with almost same reconstruction image quality.

1. Introduction

Two-dimensional (2-D) X-ray computerized tomography (CT) equipments are widely spread in industrial and medical fields, and nowadays studies on reconstruction algorithm for 3-D cone-beam acquisition system are active for more usefulness [1]. For real time observation by X-ray CT, a fast reconstruction algorithm is inevitably required in both conventional fan-beam CT and cone-beam CT.

The authors recently have proposed a fast algorithm for 2-D CT using tree-structured filter bank [2]. Feldkamp et al. [3] dealt with 3-D cone-beam acquisition system and proposed an approximation reconstruction method using a rebinning and the existing fan-beam reconstruction algorithm. The authors have also shown [4] the new algorithm is applicable to the Feldkamp method. On the other hand, for 3-D CT Grangeat [5] showed that the reprojection of measured 2-D signal coincides with the derivative of the well-known Radon transform [6], and proposed an exact 3-D reconstruction algorithm for cone-beam acquisition system. His algorithm, however, requires backprojection into 3-D space, and this processing takes so much time. This paper proposes a fast implementation method for this back-projection by use of tree-structured filter bank, and shows the proposed method works approximately 700 times faster than the direct one with almost same reconstruction image quality. Bamberger et al. were aware of filter bank application to CT [8], but since their bank was under critical sampling they did not succeed in the CT reconstruction owing to holding distortion.

In what follows, we first review the relation of cone-beam CT to Radon transform in 3-D space, and then

describe the similarity between processings of the back-projection and of synthesis in 2-D subband system. In the third place, we describe our proposed algorithm for 3-D backprojection, and evaluate the efficiency and reconstruction image quality of our algorithm comparing to the direct method.

2. Relation of Cone-beam CT to Radon Transform

Radon transform of a 3-D function $f(\mathbf{r})(\mathbf{r} \in \mathbb{R}^3)$ is defined [6] as

$$F(t, \theta) = \iiint f(\mathbf{r}) \delta(t - \theta \cdot \mathbf{r}) d\mathbf{r}, \quad (1)$$

where $\delta(t)$ denotes the 1-D Dirac delta function, θ the 3-D vector limited on the unit sphere and $\theta \cdot \mathbf{r}$ shows the vector inner product. Inverse Radon transform corresponding to

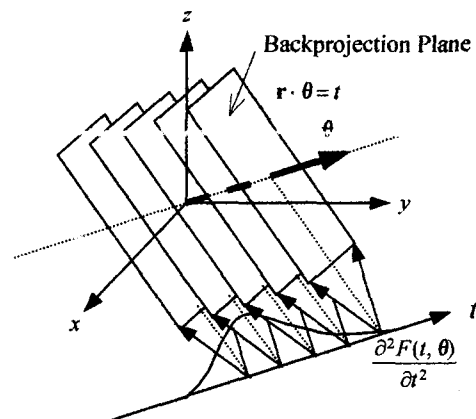


Fig.1 Illustration of Inverse Radon Transform

Eq.(1) becomes [6]

$$f(\mathbf{r}) = \iint_{|\theta|=1} \left[-\frac{d^2}{dt^2} F(t, \theta) \right]_{t=\mathbf{r} \cdot \theta} d\theta, \quad (2)$$

where $[\cdot]_{t=s}$ shows the substitution of t by s and $\iint d\theta$ the integration over the unit sphere. Fig.1 shows the interpretation to the inverse Radon transform of Eq.(2). For the given Radon transform $F(t, \theta)$ we first take the second derivative of the transform in respect to t and secondly backproject the derivative values onto the plane $\theta \cdot \mathbf{r} = t$ for each θ and t , and in the last sum up the back-projected values of all θ at every \mathbf{r} .

In cone-beam acquisition system, corresponding to a position of X-ray source we get a 2-D image on the opposite opposite face of the object. Grangeat showed that the first derivative of Radon transform coincides with reprojection of the observed image [5]. Therefore, from Eq.(2) we see that reconstruction can be carried out by taking once more the derivative of the reprojected data and backprojecting the values over the plane $\theta \cdot \mathbf{r} = t$. For realization of this method, we must devise a fast algorithm for the 3-D backprojection in Eq.(2).

3. Filter Bank Method for Backprojection

For simplicity of describing filter bank method, we restrict our discussion to two dimensions in this section.

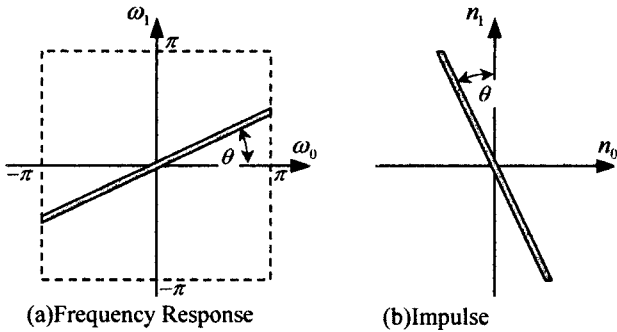


Fig.2 Responses of 2-D Narrow Bandpass Filter

At first, let us consider a very narrow 2-D bandpass filter having the frequency response shown by Fig.2(a). From the delta function property of the Fourier transform pair, the impulse response of the bandpass filter will become the one shown in Fig.2(b). Therefore, when applying this filter to the signal $x(n_0, n_1)$ such that $x(n_0, n_1) = 0$ for $n_1 \neq 0$, the nonzero values on the n_0 axis will be copied out along the direction of the impulse response, resulting in backprojection. When a 2-D signal is given over the lattice points on every horizontal line, each separated by K in the n_1 direction, and well correlated in the direction declined by θ to the n_1 axis, the above filter yields the interpolation in the θ direction by the factor K . Since the separating lattice points between the valid horizontal lines are not known in the beginning, we at first allot the zeros to these separating points (upsampling) and then make the filtering with the corresponding directional bandpass filter.

Fig.3(a) shows the passbands of K directional filters necessary for synthesis of the angular range of $-\pi/4 < \theta < \pi/4$. Their passbands overlap each other near the origin but exclude on the edges at $\omega_0 = \pm \pi$. Fig.3(b), where \mathbf{n} and \mathbf{z} respectively are the vector notations of lattice points and the Z variables, shows the block diagram of implementation of backprojection using synthesis bank for the range $-\pi/4 < \theta < \pi/4$. All signals to be synthesized are upsampled by the factor K in the n_1 direction, followed by filtering with the corresponding directional filters, and then summed up to give the synthesis signal. Since Fig.3 demonstrates the synthesis for the range $-\pi/4 < \theta < \pi/4$ only, in order to fully reconstruct the CT slice we have to carry out the same

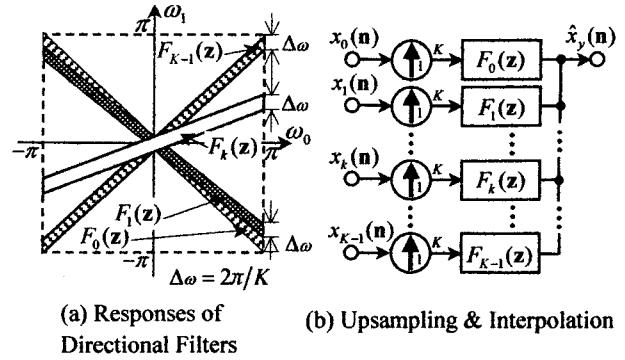


Fig.3 Illustration for Synthesis Bank for Backprojections

processing for the angular range $\pi/4 < \theta < 3\pi/4$ with exchanging n_1 and n_2 , and add the resultant signal to that of $-\pi/4 < \theta < \pi/4$.

The above processing is eventually a kind of synthesis bank in subband system [7]. When K is a power of 2, we can de-compose those directional filters into tree-structure.

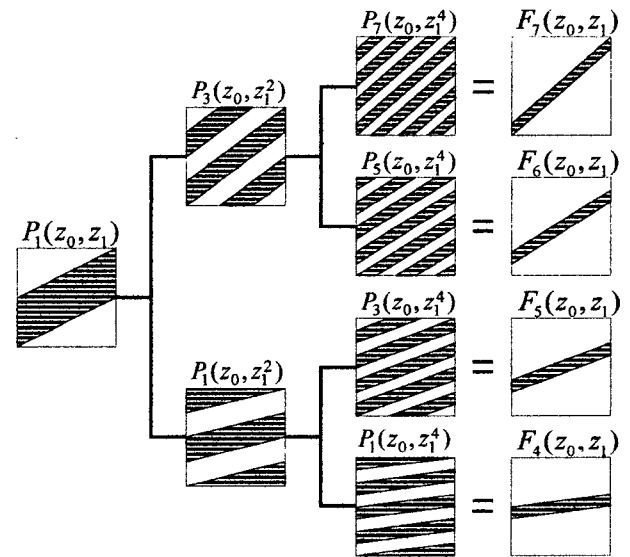


Fig.4 Tree Structure of 2-D Directional Bandpass Filter

Fig.4, which illustrates the passband of each filter, shows the tree- structure for the synthesis of the angular range $0 < \theta < \pi/4$ in the case of $K=8$. Since the common processing is executed in one time in the tree-structure, it accelerates the processing speed by the factor $K/\log_2 K$ comparing to the direct backprojection method [4]. In this bank, the variable parallelogram filter $P_k(z_0, z_1)$ works as synthesis filter [2]. $P_k(z_0, z_1)$ are given by

$$P_k(z_0, z_1) = \frac{1}{2} \left(1 + z_0^{-(1+k)/2} U(z_0) U(z_0^k z_1^2) \right); k = \text{odd}, \quad (3a)$$

where the unit filter $U(z)$ is expressed in terms of the allpass filter $A(z)$;

$$U(z) = \frac{1}{2} (zA(z) + A(z^{-1})); A(z) = \frac{1+az^{-1}}{1+az}, a = 0.5. \quad (3b)$$

This parallelogram filter can attain approximately 40dB stopband attenuation. It is noted that anticausal operations

in the above expression may be executed by time reversal [7] for finite size 2-D signal such as a CT slice.

4. Filter Bank Method for Backprojection

3-D backprojection requires 3-D narrow bandpass directional filters.

Fig.5(a) shows the implementation of such a filter in the Fourier domain. First, we apply the 2-D directional filter as shown in (b) in the $\omega_0 - \omega_1$ plane and then in the $\omega_0 - \omega_2$ plane, where the 2-D directional filters are realized in Section 3. By this direct product implementation, the resulting 3-D passband becomes their intersection as shown by the gray slab in (a). The end of this slab moves on the face parallel to the $\omega_1 - \omega_2$ plane of the cube in (a) according as the directions of the both 2-D parallelogram filters change. The 3-D filter shown in Fig.5(a) acts on the

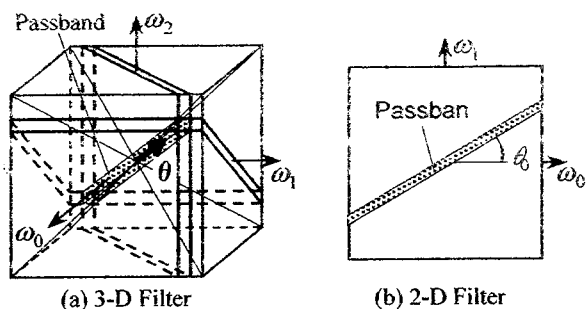


Fig.5 Direct Product Implementation of 3-D Directional Filter

3-D input at the lattice points shown by the circle in Fig.6. Specifically the second derivatives of the Radon transform is at first backprojected and interpolated at the lattice points separated by K in the n_1 and n_2 directions. We call this processing sub-projection. Then, using the 3-D directional filter, we interpolate another lattice points between the known samples. This interpolation is carried out in two steps; the first is the interpolations with the $n_0 - n_1$ coordinates in the two planes indicated by dark parallelograms in Fig.6, and the second the interpolations with the $n_0 - n_2$ coordinates in the planes perpendicular to the dark parallelogram. The former interpolations are done only for the N/K planes, but the latter for N planes, where N is the size of reconstructed 3-D image. To all the interpolations done in

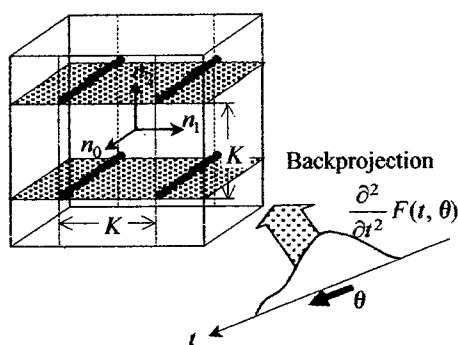


Fig.6 Initially Given Data Points and Backprojection

plane we apply the algorithm using tree-structured filter

bank mentioned in Section 3.

The above processing can be carried out for the interpo-

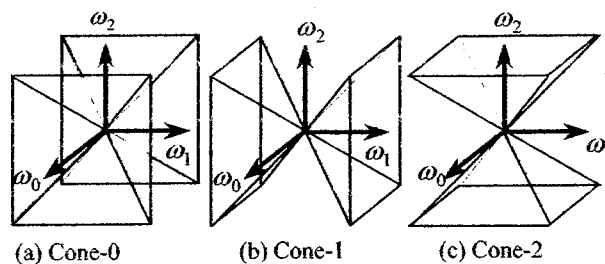


Fig.7 Direction Cones

lations of the directions included in the cone-0 shown in Fig.7(a). For full reconstruction using all direction data, we must carry out the same processing for another directions included in cone-1 and cone-2 shown in (b) and (c), respectively. The three interpolated 3-D signals are added together to get the objective 3-D reconstructed image.

5. Complexity

Suppose the size of 3-D image to be reconstructed $N \times N \times N$ pixels and the number of directions per a square cone $K^2 = (N/\kappa)^2$. The number of multiplications in the direct backprojection method is given by

$$\#_{\text{direct}} = 3 \left(\frac{N}{\kappa} \right)^2 \times N^3 = \frac{3}{\kappa^2} N^5. \quad (4)$$

Now, let us consider for the tree-structured filter bank (TSFB) method. First, the number of multiplications for the sub-projections is given by

$$3K^2 \times \left(\frac{N}{K} \right)^2 N = 3N^3. \quad (5)$$

In the second place, since the total number of repetitions of plane interpolation is $3 \times (N + K \times N/K) = 6N$ and since the number of multiplications per one plane interpolation is $3N^2 \log_2 K$ [2], the number of multiplications for TSFB interpolation is given by

$$3N^2 \log_2 K \times 6N = 18N^3 \log_2 \frac{N}{\kappa}. \quad (6)$$

The total number of multiplications is given by sum of Eq.(4) and (5).

$$\#_{\text{TSFB}} = 3N^3 \left(1 + 6 \log_2 \frac{N}{\kappa} \right) \quad (7)$$

Since we usually select $\kappa = 4$, $\#_{\text{TSFB}}$ is considered to be proportional to N^3 but N^5 . Therefore TSFB is much faster than the direct method. Moreover TSFB method has the property that memory access occurs often in consecutive addresses, and therefore processors with cache can execute TSFB in pipeline manner. In addition, since multiplication constant a in the allpass filter Eq.(3) is equal to 1/2, even if fixed point arithmetic is used instead of floating, the

reconstruction distortion may not increase so much.

5. Simulations

We conducted reconstruction simulations of TSFB and the direct methods. We used a 3-D phantom of $N \times N \times N$ pixels composed of many elliptic bodies, and simulations were performed on Pentium III (800MHz) processor using "C" language that does not support the STREAM-SIMD. $\kappa=4$ was supposed in TSFB method.

Table 1 compares the processing time. From the table

Table 1 Comparison of Processing time

N	Direct	TSFB	Ratio (Direct/TSBF)
32	4.6[sec]	0.29[sec]	17
64	2.8[min]	2.6[sec]	64
128	1.5[hour]	23.2[sec]	232
256	2.0[day]	3.8[min]	759

we see that the proposed method works approximately 700 times faster than the direct method for the usual image size $N=256$ and the ratio increases approximately as proportional as N^2 .

Fig.8 compares the reconstructed images at the position $z=-0.25$, where the size of the phantom is normalized so that the $f(x,y,z)=0$ for $|x|,|y|,|z|>1$. We see the image qualities of the direct and TSFB method are almost same. Peak signal-to-noise ratio (PSNR) is a little bit lower for TSFB method. This error is due to the poor termination processing of the allpass filter at the rim of the image. Nevertheless we can conclude TSFB is practically valuable.

6. Conclusion

In this paper we have proposed a fast implementation method for 3-D inverse Radon transform by use of tree-structured filter bank (TSFB). Inverse Radon transform is important especially in 3-D cone-beam CT. We have shown the proposed method works approximately 700 times faster than the direct one with almost same reconstruction distortion for usual image size.

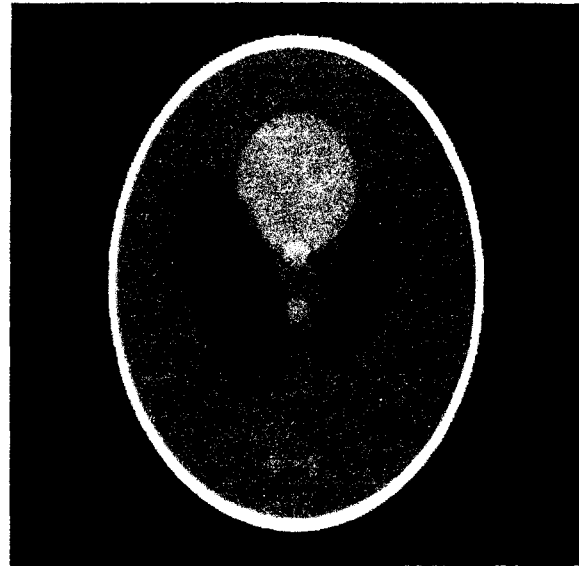
Future work will be to install TSFB into Grangeat method and to devise a clever termination method of the allpass filter.

References

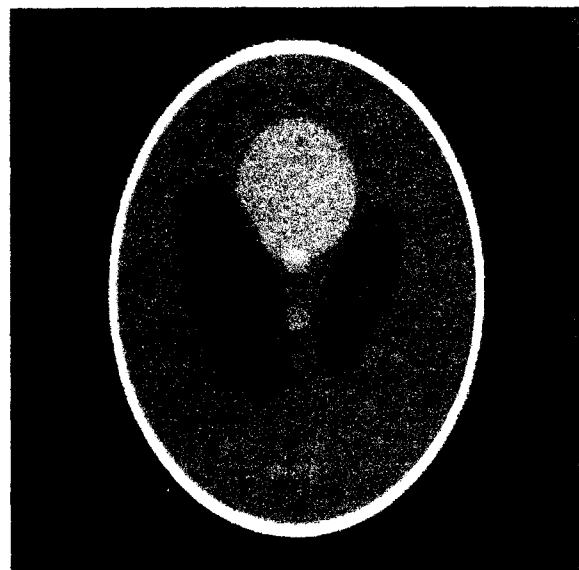
[1] C. Axelsson-Jacobson, R. Guillemaud, P.E. Danielsson, P. Grangeat, M. Defrise, and R. Clack, "Comparison of Three 3D Reconstruction Methods from Cone-Beam Data," in P. Grangeat and J. Amans (ed.), *Three-Dimensional Image Reconstruction in Radiology and Nuclear Medicine*, pp.3-19, Kluwer Academic Publishers, 1996.

[2] J. Murakami, K. Mizowaki, and Y. Morikawa, "Reconstruction Algorithm for CT Using Tree-Structured Filter Bank," *IEICE Trans. D-II*, vol. J84-D-II, no.3, pp.580-589, March 2001.

[3] L.A. Feldkamp, L.C. Davis, and J.W. Kress, "Practical Cone-Beam Algorithm," *Journal of Optical Society America A*, vol.1, no.6, pp.612-619, 1984.



(a) Direct Method (PSNR=26.4dB)



(b) TSFB Method (PSNR=25.9dB)

Fig.8 Comparison of Reconstructed Image Quality

[4] J. Murakami, K. Mizowaki, and Y. Morikawa, "Reconstruction Algorithm for Helical CT Using Tree-Structured Filter Bank," *Proc. of the 2001 Int. Tech. Conf. on Circ./Sys, Comp. and Communications*, vol.2, pp.1095-1098, July 2001.

[5] P. Grangeat, "Mathematical framework of cone beam 3D reconstruction via the first derivative of the Radon transform," in G.T. Herman, A.K. Louis and F. Natterer (ed.), *Mathematical Methods in Tomography*, Lecture Notes in Mathematics, vol.1497, pp.66-97, Springer, 1991.

[6] S.R. Deans, *The Radon Transform and Some of Its Applications*, Reprint ed. Krieger Publishing, 1993.

[7] P.P. Vaidyanathan, *Multirate Systems and Filter Banks*, Prentice Hall, 1993.

[8] R.H. Bamberger, and M.J.T. Smith, "A Filter Bank for the Directional Decomposition of Images: Theory and Design," *IEEE Trans. Signal Process.*, vol.40, no.4, pp.882-893, 1992.